

# Improving Mid-tone Quality of Variable-Coefficient Error Diffusion Using Threshold Modulation

Bingfeng Zhou\*, Xifeng Fang  
National Key Laboratory of Text Information Processing  
Institute of Computer Science and Technology  
Peking University  
Beijing, P.R.China

## Abstract

In this paper, we describe the use of threshold modulation to remove the visual artifacts contained in the variable-coefficient error-diffusion algorithm. To obtain a suitable parameter set for the threshold modulation, a cost function used for the search of optimal parameters is designed. An optimal diffusion parameter set, as well as the corresponding threshold modulation strength values, is thus obtained. Experiments over this new set of parameters show that, compared with the original variable-coefficient error-diffusion algorithm, threshold modulation can remove visual anomalies more effectively. The result of the new algorithm is an artifact-free halftoning in the full range of intensities. Fourier analysis of the experimental results further support this conclusion.

**Keywords:** Halftoning, Error-Diffusion, Correlation, Fourier Transform, Blue Noise, Threshold Modulation

## 1 Introduction

The error-diffusion algorithm is a very important method for generating halftone images. The principle of this algorithm is to compensate the quantization errors by distributing them on to the neighboring pixels of the input image. The original error-diffusion algorithm scans pixels of the input image in a top-down, left-to-right order. During the scan, each pixel is quantized by a fixed threshold value at the middle of the density range. After the quantization, the quantization error is calculated and the error is distributed by adding it to the neighboring un-processed pixels using a set of fixed distribution coefficients (see Fig.2). Detailed description and analysis of this algorithm can be found in [Knox 1999], [Ulichney 1987; 1988] and [Kang 1999]. This algorithm has lead to many research efforts due to its simplicity and effectiveness as well as its good halftoning quality. It has a wide range of applications, not only in the areas of image printing and display but also in other domains of computer graphics as illustrated by the polygonal re-meshing of Alliez et al [Alliez et al. 2002]. The blue noise feature of this algorithm also suggests its application in antialiasing of sampled images [Dippé and Wold 1985; Mitchell 1987].

Among those who contributed to the analysis and improvement of the algorithm, Ulichney introduced the “blue noise concept” [Ulichney 1988], a powerful tool for the measurement of the quality of the algorithm. The blue noise concept uses the power spectrum of the Fourier transform<sup>1</sup> of a halftone image to measure its quality. For a quality output of the error-diffusion algorithm, the dots in the generated binary image are scattered both randomly and evenly. This property, when reflected in the Fourier transform of the binary image, is characterized by a symmetrical frequency spectrum that lacks low frequencies. This defines the so-called blue noise spectrum. If the power spectrum of a binary image is calculated, it can then be compared with an “ideal blue noise spectrum”. The closer the spectrum to the “ideal blue noise spectrum” is, the better the quality of halftone image will be [Ulichney 1988; Mitsa and Parker 1992].

Based on this concept, many efforts were made to improve the output quality of the error-diffusion algorithm. Among these efforts, some notable ones are Knox’s threshold modulation [Knox 1993], Ulichney’s serpentine error diffusion [Ulichney 1987] and recently Ostromoukhov’s variable-coefficient error-diffusion algorithm [Ostromoukhov 2001; Jodoin and Ostromoukhov 2002]. In Knox’s work, an analysis model was devised based on Ulichney’s theory to analyze the effect of the threshold modulation. The serpentine method applies a back and fourth parsing order to eliminate the “worms” in light tones. Although improvements have been made by these methods, problems still exist. Among those problems, artifacts and transient effects are the most notable ones.

In 2001, Ostromoukhov presented a new improvement to the error-diffusion algorithm [2001]. In this work, he employed a variable-coefficient error-diffusion method to generate halftone images. For each important density level (key level), an optimization method is used to search for the optimal coefficients and in this way a set of diffusion coefficients are obtained. Ostromoukhov’s result improved the quality of the image dramatically, especially in the light tone area of the image. But the quality in the mid-tones can still be improved. Some artifacts still exist and the frequency spectra of these generated halftone images are also not ideal (Fig.3 (a) and (b)).

In this paper, we apply threshold modulation to the variable-coefficient error-diffusion method [Ostromoukhov 2001]. We modulate the threshold by adding a random perturbation into the original fixed threshold value of Ostromoukhov’s algorithm. By controlling the amplitude of random perturbation<sup>2</sup> for each density level, better error-diffusion output is obtained. In the following

---

\*E-mail: cczbf@pku.edu.cn

Permission to make digital/hard copy of part of all of this work for personal or classroom use is granted without fee provided that the copies are not made or distributed for profit or commercial advantage, the copyright notice, the title of the publication, and its date appear, and notice is given that copying is by permission of ACM, Inc. To copy otherwise, to republish, to post on servers, or to redistribute to lists, requires prior specific permission and/or a fee.  
© 2003 ACM 0730-0301/03/0700-0437 \$5.00

---

<sup>1</sup>In this paper, *power spectrum* of the Fourier transform is also referred to as *frequency spectrum*

<sup>2</sup>In this paper, *amplitude of random perturbation* is also referred to as *modulation strength*

sections, the effect of threshold modulation on Ostromoukhov's algorithm is examined. Then, a cost function, which is based on the blue noise theory [Ulichney 1987; 1988], is designed for the search of the best coefficients when the threshold modulation is applied. The coefficients and modulation strengths obtained for key density levels by optimal value search are presented. The output results corresponding to these parameters are analyzed and compared with those of Ostromoukhov's algorithm and other advanced techniques.

## 2 Threshold Modulation

Ostromoukhov's variable coefficient method has dramatically improved the output quality of the error-diffusion algorithm. His work also suggested an optimization method for searching for the best coefficients under a cost function. Using the coefficients given in Ostromoukhov's paper [2001], image qualities, especially in light tones, are improved, but there still exist some problems.

The problems that Ostromoukhov's work [2001] does not solve can be classified into two kinds. The first kind is "visible artifacts". "Visible artifacts" appear in the light-tones of the output image as "worm effects" and "visually harmful alignment" in mid-tones (See Fig.3 (a)). Ostromoukhov's coefficient set eliminates "worm effects" effectively, but it does not noticeably improve "visually harmful alignment" around mid tones (see Fig.3 (a) and (b)).

The second kind of the problems is "transient effects". They appear around drastic changes in the density of the input image. When these changes occur, the structure of dot distribution in the changing area appears non-stable. The non-stables structure stretches out until it reaches the area that is far from the input density discontinuity. Then the unstable structure disappears and the image maintains a stable and uniform dot distribution (See Fig.5(c)). Again, Ostromoukhov's algorithm works for this effect in the light tone area but does not work well in the mid-tone area.

If we investigate the Fourier frequency spectrum of an output image containing "visible artifacts" or "transient effects", it can be found that the spectrum takes a quite different shape from the "ideal blue noise spectrum" (See Fig.3 (b) and (d)). This is the reason why the "visible artifacts" and "transient effect" are so objectionable to human eyes. Thus, to eliminate these visually objectionable artifacts, the frequency spectrum must be forced to be closer to the round shaped and symmetrical "ideal blue noise spectrum". To achieve this goal, it is straightforward to apply the threshold modulation suggested by Ulichney [1987; 1988] and analyzed by Knox [1993] directly to Ostromoukhov's variable-coefficient algorithm. In our experiment, the threshold function is calculated using a white noise random number generator, and the equation of threshold function containing the threshold modulation is as follows:

$$t(i) = 128 + (\text{rand}(x, y) \bmod 128) \cdot m(i) \quad (1)$$

where  $\text{rand}(x, y)$  is the white noise random number generator<sup>3</sup>,  $(x, y)$  is the position of the pixel in input image,  $i \in [0, 255]$  is the density level of the pixel of the input image, and  $m(i) \in [0.0, 1.0]$  is modulation strength. In our initial experiment, Ostromoukhov's

<sup>3</sup>The random number generator can be implemented using the program library supplied with any programming languages such as c++.

algorithm and its coefficient set are used [2001]. The algorithm is used unchanged except that the threshold is modulated using Eq. (1) and the effect of the modulation is shown in Fig.3(c) and (d).

By comparing Fig.3 (c) with Fig.3 (a), which is the output image generated using Ostromoukhov's original variable-coefficient algorithm [2001], significant improvement can be found in Fig.3(c). In Fig.3 (a), horizontal anomalies can be seen clearly, but in Fig.3(c), these horizontal anomalies are replaced by evenly scattered "chess board" and "horizontal bar" patterns. These patterns are visible, but they are much less objectionable than those contained in Fig.3 (a).

The comparison shows that threshold modulation is an effective way to reduce the visible anomalies. Despite this improvement, the result is not yet perfect. First, anomalies are still visible, the "vertical bar" pattern and "chess board" patterns appear alternatively with a relatively large area. Second, the frequency spectrum of the generated image is not symmetrical, albeit it appears closer to the "ideal blue noise frequency spectrum" than the one shown in Fig.3 (b), possibly due to the large portion of the "vertical bar" patterns contained in the resulted image.

To obtain a better distribution, the frequency spectrum of the output image should have a symmetric shape, and this can be achieved by the search for the most suitable coefficients of the error-diffusion filter [Press et al. 1992; Ostromoukhov 2001]. In the following sections, a corresponding cost function will be described with its result presented and analyzed.

## 3 Searching for Optimal Coefficients

As described in the last section, the error-diffusion coefficients obtained by Ostromoukhov are not optimal in the presence of the threshold modulation. To search for the optimal coefficients, the threshold modulation must be included in the standard error-diffusion algorithm. As in Ostromoukhov's work [2001], a simplex method [Press et al.1992] is used for the search for optimal diffusion coefficients. In this search, the threshold modulation defined in Eq. (1) is applied to the error-diffusion algorithm given in [Ostromoukhov 2001]. After the diffusion coefficients are obtained by the search, the modulation strength  $m(i)$  is fine-tuned manually and then finalized into our optimal parameter set (Table 1 and 2) which can be used in the halftoning process of the algorithm.

When performing the search for optimal parameters, the optimization target is to obtain the symmetrical frequency spectrum that is as close as possible to the "ideal frequency spectrum". The cost function of the search is the key to achieve this target. In our work, the cost function is the sum of two parts (Eq. (4)). The first part measures the symmetry of the spectrum. The second part measures the similarity of the spectrum to the "ideal frequency spectrum".

In the first part, the concept of *radially averaged power spectrum* as defined in [Ulichney 1988] is employed but in a segmented way. That is, three *segmented radially averaged power spectrum*, as defined in Eq. (2), are calculated for the three directions in the frequency spectrum as illustrated in Fig.1. Then, the correlation [Castleman 1996] of these three power spectrums is calculated. This correlation is used as the first part of the cost function, which is contributed by the symmetry of the target frequency spectrum.

The segmented radially averaged power spectrums are defined in Eq. (2) as following:

$$\begin{aligned}
P_0(f_r) &= \frac{1}{N_0(f_r)} \sum_{i=1}^{N_0(f_r)} \tilde{P}(f) \\
P_{45}(f_r) &= \frac{1}{N_{45}(f_r)} \sum_{i=1}^{N_{45}(f_r)} \tilde{P}(f) \\
P_{90}(f_r) &= \frac{1}{N_{90}(f_r)} \sum_{i=1}^{N_{90}(f_r)} \tilde{P}(f)
\end{aligned} \quad (2)$$

where  $P_0$ ,  $P_{45}$ ,  $P_{90}$  are three segmented radially averaged power spectra corresponding to the three areas defined in Fig.1;  $N_0(f_r)$ ,  $N_{45}(f_r)$ ,  $N_{90}(f_r)$  denote the number of frequency samples in the frequency spectrum along the annulus of radius  $r$  but falls in to vertical, diagonal and horizontal segments respectively.  $P(f)$  is the frequency spectrum estimate as defined in [Ulichney 1988].

Another part of our cost function concerns the similarity of the target frequency spectrum to the “ideal frequency spectrum”, which is calculated as the ratio between the area covered by the radially averaged power spectrum curve  $P(f)$  [Ulichney 1988] below the principal frequency and the total area covered by the whole curve (See Eq.(3) and Fig.1). This *low frequency ratio* for a halftone image with a density level of  $g$  is denoted as  $L(g)$  and can be presented by Eq.(3):

$$L(g) = \frac{\int_0^{f_p} P(f) df}{\int_0^{1/\sqrt{2}} P(f) df} \quad (3)$$

After the two parts of the cost function are obtained, the cost function is calculated as a weighted sum of the two parts (Eq.(4)):

$$C(g) = \text{Corre}(P_0^{(g)}, P_{45}^{(g)}, P_{90}^{(g)}) \cdot w + L(g) \cdot (1-w) \quad (4)$$

where  $g$  is the density level of the halftone image being considered,  $P_0^{(g)}$ ,  $P_{45}^{(g)}$ ,  $P_{90}^{(g)}$  are the segmented radially averaged power spectra of the frequency spectrum of the halftone image at density level  $g$ .  $w$  is the weight ( $0 \leq w \leq 1$ ) and is decided according to the convergence of our parameter search. *Corre* is the correlation function of the three curves  $P_0^{(g)}$ ,  $P_{45}^{(g)}$ ,  $P_{90}^{(g)}$  and the larger its value is, the less similar the three curves are. Given this definition, the target of the search is thus to find the appropriate coefficients for a given density level so that they minimize the cost function.

## 4 Results

Using the cost function defined in Eq. (4), a set of key parameters can be found. The density levels of key parameters are chosen by a visual inspection of the output of Ostromoukhov's variable coefficient algorithm, as illustrated in Fig.4 (a) and (c), which are halftoned from two gray scale images. The densities of the two images all range from 0 to 0.5.

In Fig.4 (a) and (c), certain density levels appear to not be good enough. For instance, in Fig.4 (a), visual anomalies appear at level 127/255 and 79/255, transient effects exist at the edge of the image at level 44/255. When deciding which density levels are chosen as the key levels of our parameter set, we first add all Ostromoukhov's key levels into our set. Then, those levels that are not ideal and do not exist in Ostromoukhov's key parameter set are added.

Before performing the search for optimal parameters for a key density level, the threshold modulation strength  $m(i)$  is set to its max value (Eq. (1)), and then the search for the optimal diffusion coefficients is performed. After the diffusion coefficients for that density level are found (Table. 1) and the sample halftoning result is obtained, the modulation strength  $m(i)$  is adjusted manually to further reduce the low frequency component contained in the frequency spectrum of the results while keeping the “blue noise” property of the output image. The adjustment is done with reference to the corresponding output image and its frequency spectrum. By performing the same operations for each key level, a diffusion coefficient set and a parameter set of  $m$  are obtained and listed in Table 1 and Table 2 respectively. When using the parameter set of Table 2, modulation strength  $m(i)$  that goes in-between the two key values is decided, just like the in-between diffusion coefficients, by a linear interpolation.

After the diffusion coefficients and threshold modulation strength values were determined, a series of comparisons was made between our algorithm and Ostromoukhov's. Fig.4, 5, and 6 are some of the results.

Among these results, significant improvement, especially with respect to the “visible artifact” and “transient effect”, can be found in Fig.4 (b) and (d) in the full range of the densities. In Fig.5, besides the better visual appearance of the results of our algorithm, better symmetries can be found in the frequency. The similarity of the shape of the three segmented radially averaged power spectra proves the effectiveness of the designing of our cost function.

In Fig.6, 7 and 8, results of experiments on continuous-tone images, as well as the comparison of our result with other halftoning techniques, are illustrated. In these results, “visible artifacts” can be found in the mid-tone area (e.g.: in the upper-right portion of the images in Fig.7) in the output of most of other error-diffusion algorithms but are removed from the result of ours.

## 5 Analysis and Conclusions

In this paper, threshold modulation using a white noise random sequence is introduced into the variable-coefficient error diffusion. According to the analysis made by Knox [1993], adding white noise to the threshold of standard error-diffusion algorithm is equivalent to first adding to the input image a noise that is high-pass filtered from the same white noise used in the threshold modulation, and then halftoning the modified image by a standard error-diffusion where the threshold is constant. According to Ulichney's blue noise concept, the high-pass filtered white noise is precisely the blue noise where harmful low frequency components are reduced. So adding white noise to the threshold may not cause grainy effect in the area where the threshold modulation is applied. Notice the background of the flowers and glass in the images of Fig.7, the original visible irregular vertical patterns ((b), (c) and (f)) are replaced by the evenly distributed fine patterns, where no trace of irregular dot clustering, a major cause of granularity, can be found.

As analyzed above, threshold modulation is a kind of high frequency perturbation to the error-diffusion result, and this perturbation must not affect the ideal blue noise property of the output, which means that the threshold modulation must be applied in a controlled way. To achieve this goal, we introduced the concept of modulation strength. By controlling the level of the

modulation strength, an optimal halftoning result, as illustrated in our experiment result, can be achieved.

In the presence of the controlled threshold modulation as described above, by searching for optimal values of the coefficients using the cost function presented in this paper, a set of the diffusion coefficients and threshold modulation strengths with a nearly-optimal mid-tone performance is obtained (Table 1, Table 2)<sup>4</sup>. The experimental results of this set of parameters show that, while keeping the simplicity of the original algorithm, the method described in this paper is effective for removing most visual anomalies remaining in Ostromoukhov's results. Compared with another similar work about *tone dependent error diffusion* [Li and Allebach 2002], our algorithm and optimization model are simpler. We expect that the simplicity of our method may bring about flexibility and efficiency in its implementation.

In our experiment, modulation strength is obtained manually rather than in a combined "global" search. There are two reasons for doing so. First, there are no guidelines for finding a good initial estimate for the combined search for optimal values of parameters and furthermore, adding one more parameter ( $m(i)$ ) into the searching process will decrease the efficiency of the search. These two factors may lead to the failure of the search. Second, fine tuning a single parameter  $m(i)$  with the reference of the power spectrum will not decrease the efficiency of the experiment and the optimal value of  $m(i)$  can be easily obtained with a single experiment. For these reasons, we believed that manual adjustment in finding the modulation strength  $m(i)$  is a feasible and effective way to perform our experiment. The results of the experiment proved the validity of this method. A drawback of manual adjustment is that the resulting modulation strength is "nearly optimal" in theory. If an automatic search is preferred, we suggest performing the diffusion coefficients search first, then searching for the single parameter of modulation strength automatically.

## Acknowledgements

The authors would like to thank their colleagues Bin Yang and Haifeng Li. Without their beneficial discussion with the authors about the quality issues of digital halftoning, the results of this work may not have been achieved.

Thanks also to Robert Ulichney, Jan Allebach, Zhigang Fan and Gabriel Marcu for providing the reference images used in figures.

## References

- ALLIEZ, P., MEYER, M. AND DESBRUN, M. 2002. Interactive Geometry Remeshing. In *ACM Transactions on Graphics (Proceedings of ACM SIGGRAPH 2002)*, 21, 3, 347-354.
- CASTLEMAN, K.R. 1996. *Digital Image Processing*, Prentice Hall, Inc.
- DIPPÉ, M.A.Z., AND WOLD, E.H. 1985. Antialiasing through Stochastic Sampling. In *Computer Graphics (Proceedings of SIGGRAPH 85)*, 19, 3 ACM, 69-78.
- FLOYD, R. W. AND STEINBERG, L. 1976. An Adaptive Algorithm for Spatial Gray Scale, *Proc. Soc. Inf. Display* 17, 75-77.

<sup>4</sup>Our parameter set and error-diffusion implementation are open for the public domain and are available from:  
<http://pccms.pku.edu.cn/~cczbf/TMErrorD>

- JODOIN, P., AND OSTROMOUKHOV, V. 2002. Error-Diffusion with Blue-Noise Properties for Midtones, *SPIE 4663*, 293-301.
- KANG, H.R. 1999. *Digital Color Halftoning*, SPIE Press, 1999.
- KIM, S. H. AND ALLEBACH, J. P. 2002. Impact of HVS Models on Model-based Halftoning, *IEEE Transactions on Image Processing*, 11,3, 258-269.
- KNOX, K.T. 1999. Evolution of Error Diffusion, *Journal of Electronic Imaging*, 8, 4, 422-429.
- KNOX, K.T. 1993. Threshold Modulation in Error Diffusion, *Journal of Electronic Imaging*, 2, 3, 185-193.
- LI, P. AND ALLEBACH, J. P. 2002. Tone-dependent Error Diffusion, In *Proc. of SPIE, Vol.4663 (2002)*, 310-321.
- MARCU, G. 2000. An Error Diffusion Algorithm with Output Position Constraints for Homogeneous Highlights and Shadow Dot Distribution. *Journal of Electronic Imaging*, 9,1, 46-51.
- MITCHELL, D.P. 1987. Generating Antialiased Images at Low Sampling Densities. In *Computer Graphics (Proceedings of ACM SIGGRAPH 87)*, 21, 4, ACM, 65-72.
- MITSA, T. AND PARKER, K.J. 1992. Digital Halftoning Using a Blue-noise Mask. *Journal of the Optical Society of America*, 9(11), 1920-1929.
- OSTROMOUKHOV, V. 2001. A Simple and Efficient Error-Diffusion Algorithm. In *Proceedings of SIGGRAPH 2001*, ACM Press / ACM SIGGRAPH, New York, E. Fiume, Ed., Computer Graphics Proceedings, Annual Conference Series, ACM, 567-572.
- PRESS, W. H., TEUKOLSKY, S. A., VETTERLING, S. A. AND FLANNERY, B.P. 1992. *Numerical Recipe In C*, Cambridge University Press.
- SHIAU, J. AND FAN, Z. 1996. A Set of Easily Implementable Coefficients in Error Diffusion with Reduced Worm Artifacts, *SPIE, Vol.2658*, 222-225.
- ULICHNEY, R. 1987. *Digital Halftoning*, MIT Press.
- ULICHNEY, R. 1988. Dithering with Blue Noise, *Proceedings Of the IEEE*, 76, 1, 56-79.
- ULICHNEY, R. 1993. The Void-and-cluster Method for Dither Array Generation. *SPIE, Vol.1913*, 332-343.
- ULICHNEY, R. 2000. A Review of Halftoning Techniques, *SPIE*, 3963, 378-391.

Table2: Key levels of threshold modulation and the modulation strengths (obtained when  $w=1.0$ ):

Key Level	Modulation strength
0	0.00
44	0.34
64	0.50
85	1.00
95	0.17
102	0.50
107	0.70
112	0.79
127	1.00

Table 1: Key levels and their diffusion coefficients (obtained when  $w=1.0$ ), the notation is defined by Ostromoukhov's paper [Ostromoukhov 2001], namely:  $A_{10}$ ,  $A_{11}$ ,  $A_{01}$  are for the input levels  $i$  in the range  $[0,127]$ ,  $d_{10}=A_{10}(i)/M(i)$ ;  $d_{11}=A_{11}(i)/M(i)$ ;  $d_{01}=A_{01}(i)/M(i)$ ,  $D(i)=\{d_{10}(i), d_{11}(i), d_{01}(i)\}=D(255-i)$  and  $M(i)=A_{10}(i)+A_{11}(i)+A_{01}(i)$

Key Level	$A_{10}$	$A_{11}$	$A_{01}$
0	13	0	5
1	1300249	0	499250
2	214114	287	99357
3	351854	0	199965
4	801100	0	490999
10	704075	297466	303694
22	46613	31917	21469
32	47482	30617	21900
44	43024	42131	14826
64	36411	43219	20369
72	38477	53843	7678
77	40503	51547	7948
85	35865	34108	30026
95	34117	36899	28983
102	35464	35049	29485
107	16477	18810	14712
112	33360	37954	28685
127	35269	36066	28664

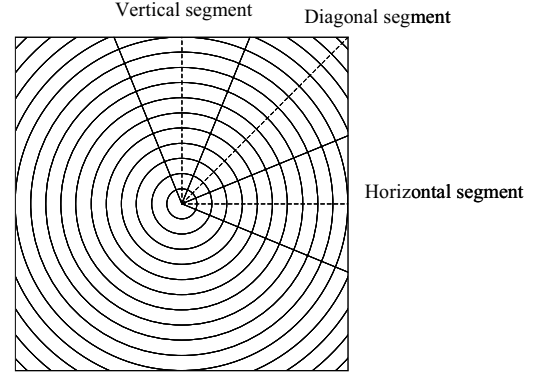


Figure 1: Three segments in the frequency spectrum are selected along vertical, diagonal and horizontal direction respectively for the three curves of segmented radially averaged power spectrums along these directions.

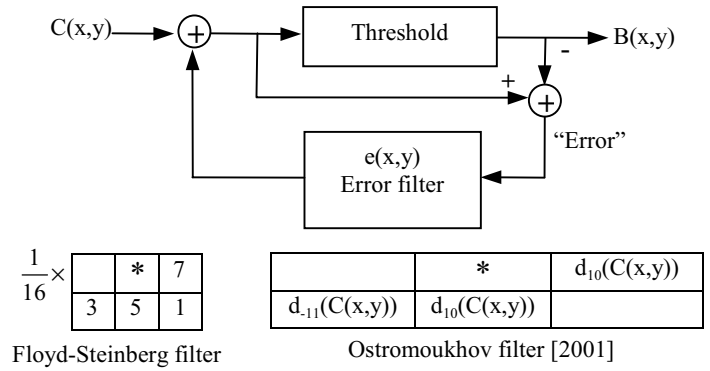


Figure 2: Error diffusion with different error filters

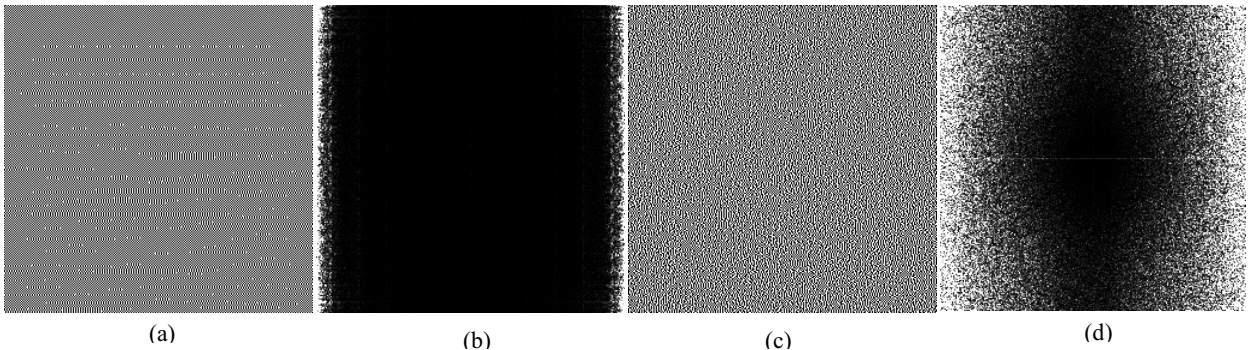


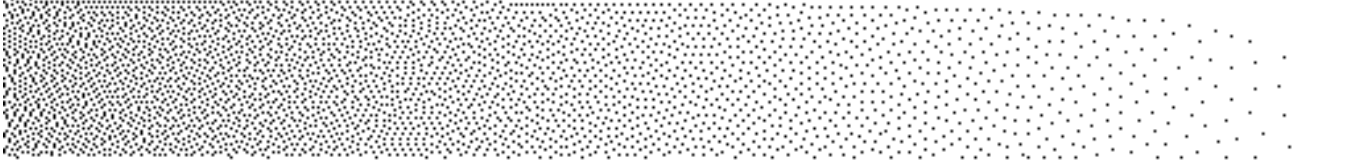
Figure 3: Effects of threshold modulation on error diffusion. (a) Half-tone image obtained using Ostromoukhov's method [2001]; (b) Frequency spectrum of (a); (c) Half-tone image obtained using Ostromoukhov's coefficients but with threshold modulation ( $m=1.0$ ); (d) Frequency spectrum of (c). Density of both half-tone images is  $127/255$  or  $0.5$ .

127/255

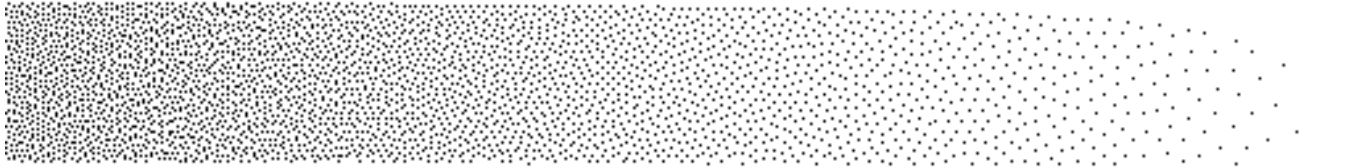
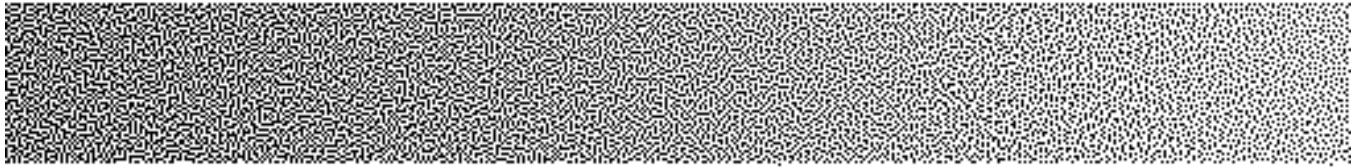
76/255



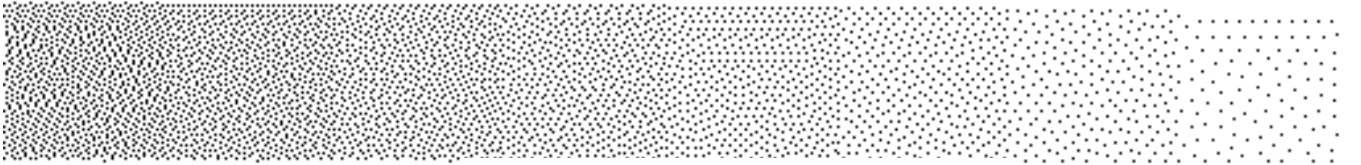
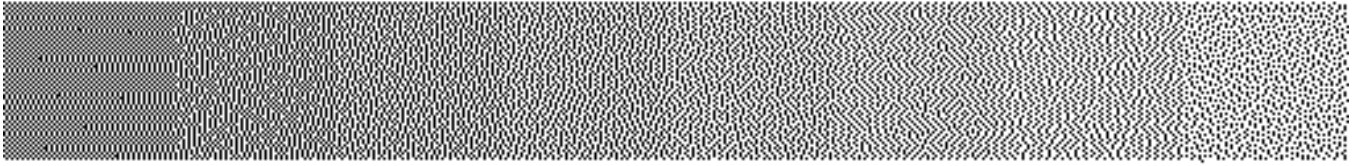
44/255



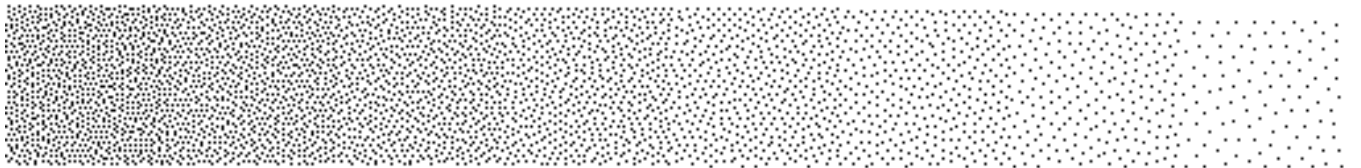
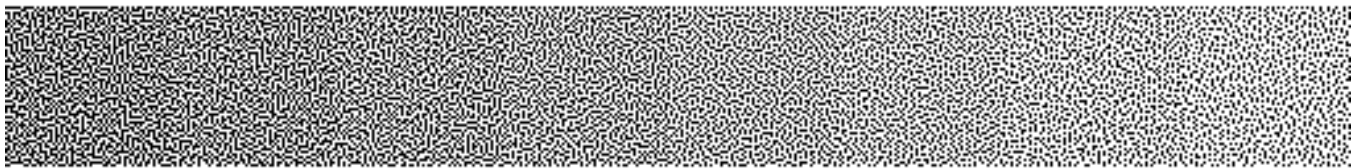
(a) Continuous ramp: Ostromoukhov's parameter



(b) Continuous ramp: Our parameter



(c) 16-step ramp: Ostromoukhov's parameter



(d) 16-step ramp: Our parameter

Figure 4: A ramp comparison between our result and Ostromoukhov's Result [2001]



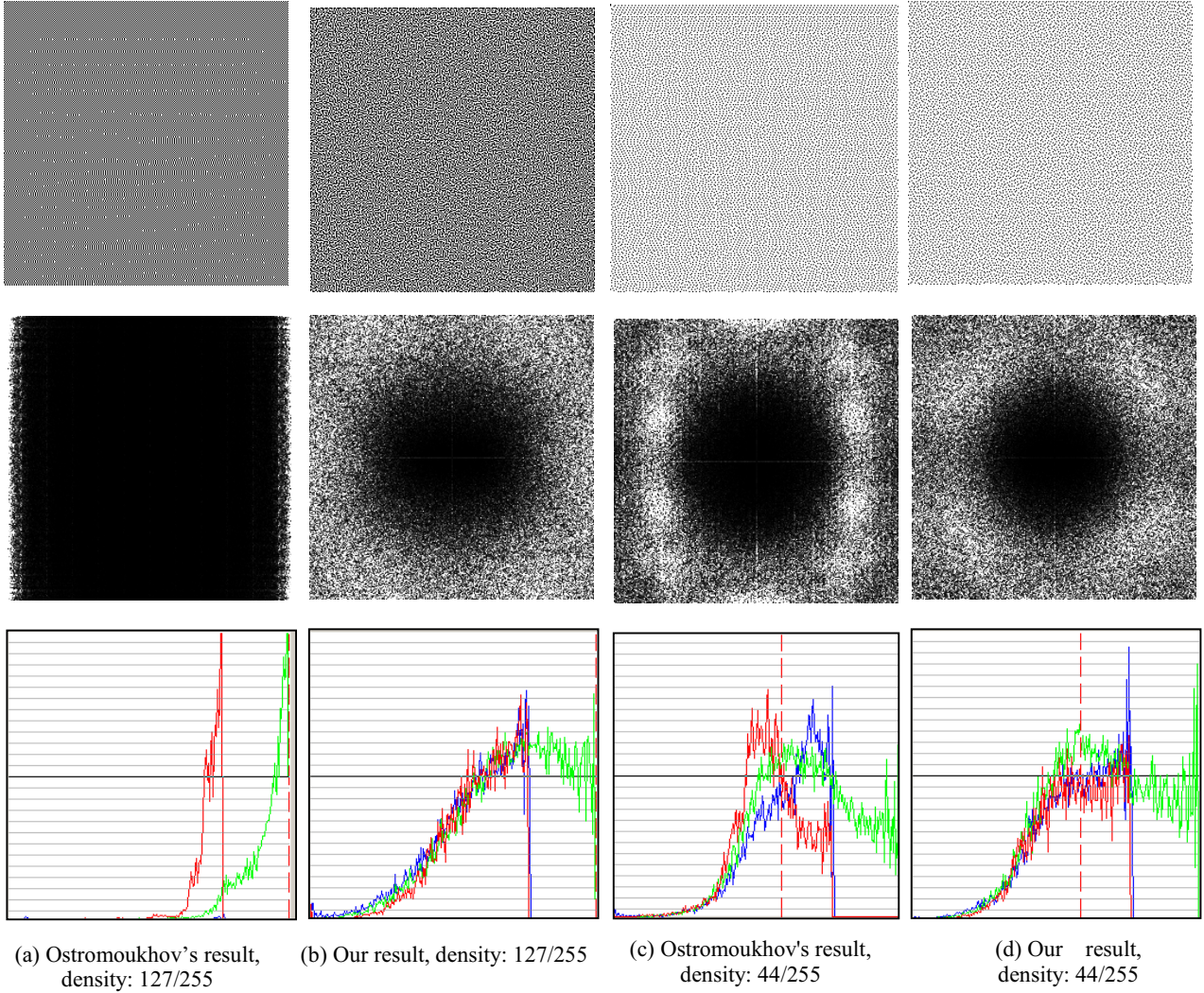


Figure 5: Comparison of the halftoning results of uniform patches with two different densities. **Top**: halftoning result. **Middle**: frequency spectrum of the result. **Bottom**: segmented radially averaged power spectrum (red: horizontal, green: diagonal, blue: vertical)

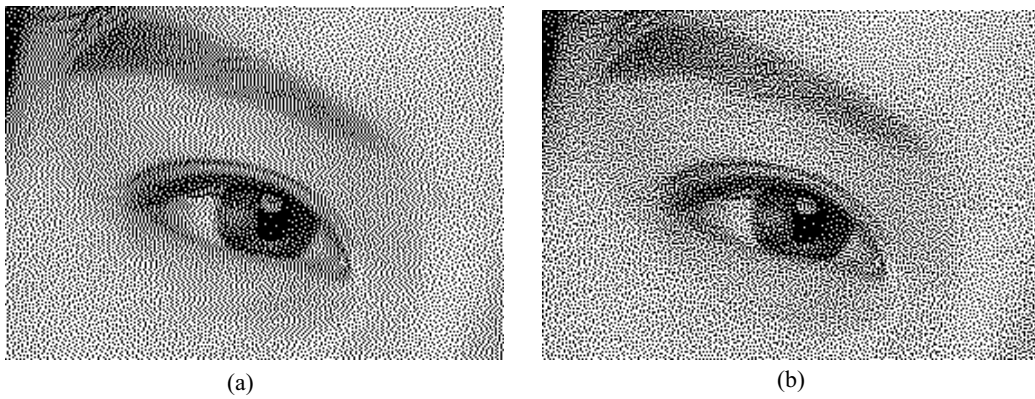


Figure 6: A comparison using continuous tone image. (a) Using Ostromoukhov's parameter; (b): Using our parameter

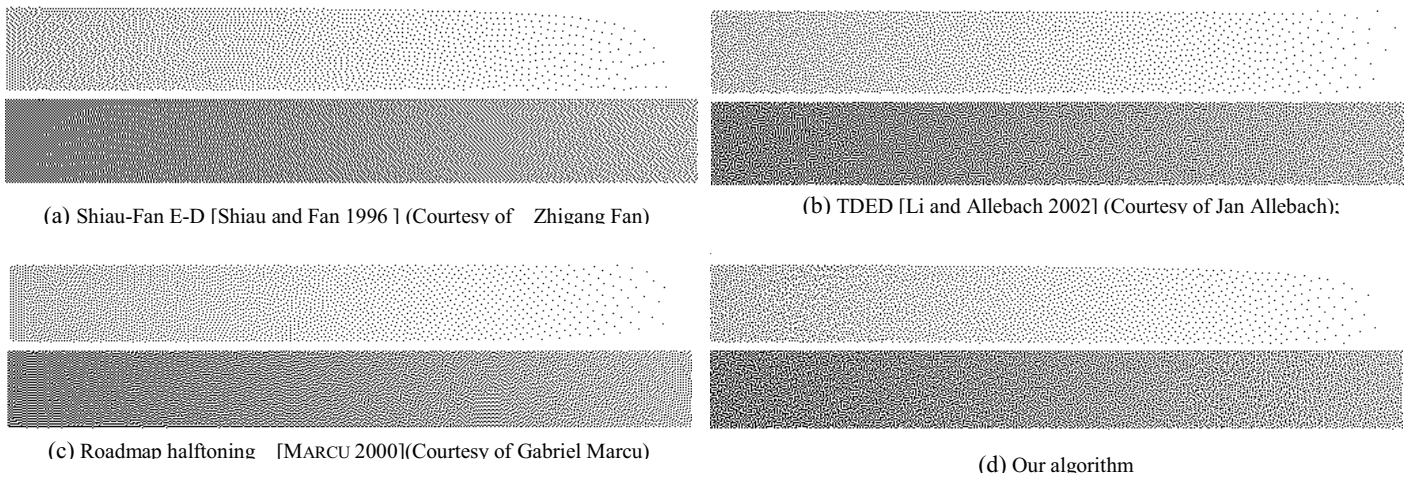
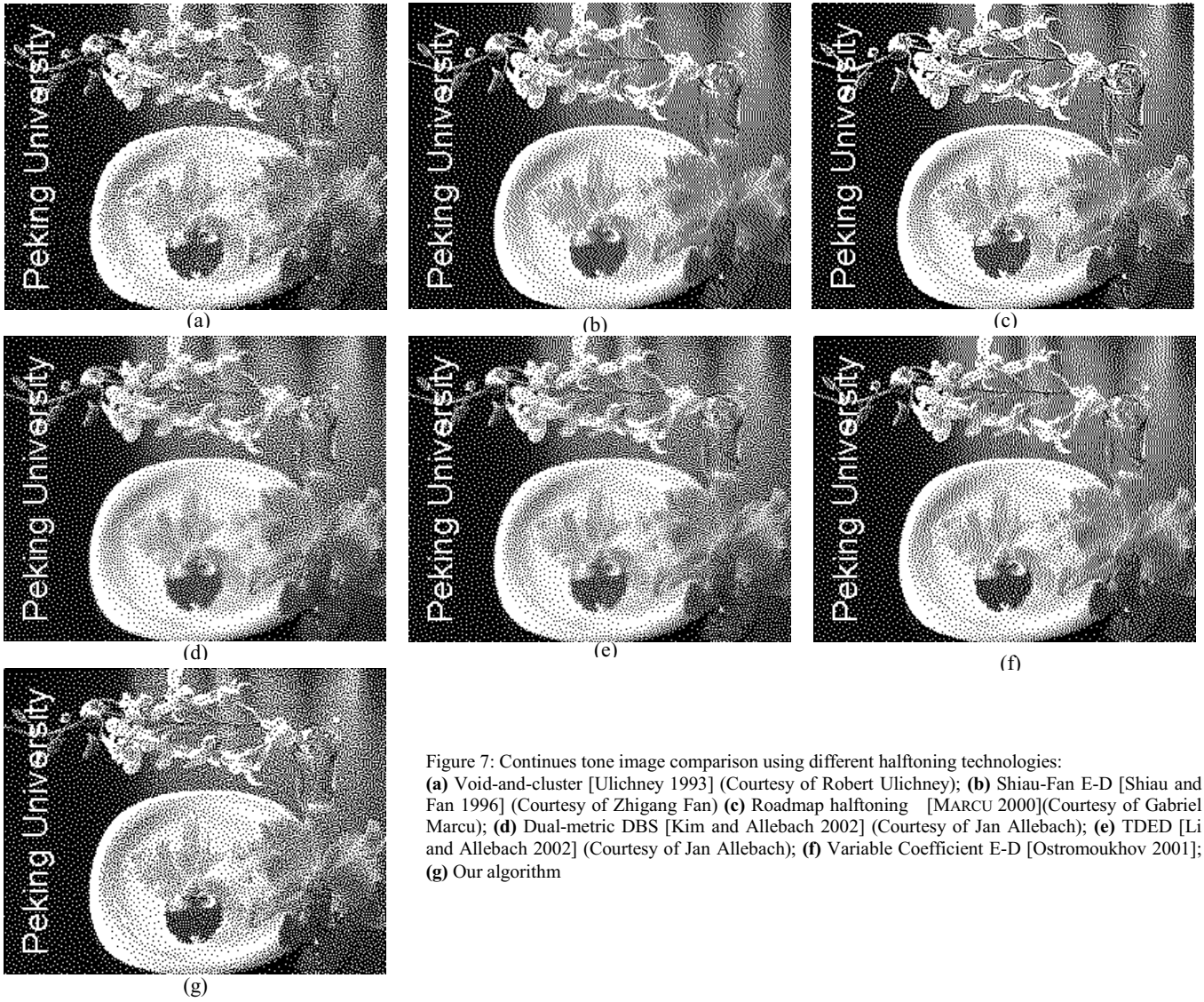


Figure 8: Ramp comparisons with other advanced E-D algorithm